Quasi-biennial oscillation disrupted by abnormal Southern Hemisphere stratosphere

James A. Anstey[1]*, Timothy P. Banyard[2], Neal Butchart[3], Lawrence Coy[4,5], Paul A. Newman[4], Scott Osprey[6,7], Corwin Wright[2]

[1]Canadian Centre for Climate Modelling and Analysis, Environment and Climate Change Canada, Victoria, Canada

[2]Centre for Space, Atmospheric and Oceanic Science, University of Bath, Bath, UK

[3]Met Office Hadley Centre, Reading, United Kingdom

[4]NASA Goddard Space Flight Center Greenbelt, Maryland, USA

[5]SSAI, Lanham, Maryland, USA

[6]National Centre for Atmospheric Science, Oxford, United Kingdom

[7]Department of Physics, University of Oxford, Oxford, United Kingdom

Corresponding author: James Anstey, `james.anstey@canada.ca`

Abstract

The quasi-biennial oscillation (QBO) is a repeating cycle of tropical stratosphere winds reversing direction from eastward to westward roughly every 14 months[1]. Discovered independently by British[2] and American[3] scientists the QBO continued undisturbed for 27 cycles from 1953 until February 2016 when a westward jet unexpectedly formed in the lower stratosphere during the eastward phase[4,5]. This disruption is attributed to unusually high wave momentum fluxes from the Northern Hemisphere[5,6]. A second, similar, QBO disruption occurred during the 2019/2020 northern winter though this time the Arctic polar vortex was exceptionally strong and wave fluxes weak[7]. Here we show that this latest disruption to the regular QBO cycling was twice as strong as that seen in 2016 and resulted from horizontal momentum transport from the Southern Hemisphere. The disruption began in September 2019 when there was a rare Southern Hemisphere sudden stratospheric warming followed by abnormal conditions in the stratosphere with the smallest ozone hole since its discovery[8,9] and enhanced equatorward momentum fluxes. In both disruptions the normal downward progression of the QBO halts and the eastward shear zone above the disruption moves upward assisted by stronger tropical upwelling during the boreal winter. Results from the two disruptions provide compelling evidence of a fundamental change in our understanding of the dynamics of the QBO with extratropical influences more significant than previously thought. In turn, this implies a less predictable QBO. Furthermore, the expected climate response of the mechanism we have identified suggests that reoccurring QBO disruptions are consistent with an emerging signal of climate change weakening QBO amplitudes as predicted by models[10–12].

Main

The QBO consists of alternating layers of eastward and westward wind that emerge above 40 km and gradually descend through the tropical stratosphere before dissipating near the tropopause (16 km)[13]. Observed periods range from 22 to 35 months averaging around 28 months[14]. The QBO dominates stratospheric variability in the tropics while modulating variability in mid to high latitudes[15] and thereby providing a useful source of predictability on seasonal-to-decadal timescales[16]. The established QBO fluid dynamical mechanism involves vertically propagating waves from the troposphere that accelerate the winds through interactions with the winds themselves[1]. This leads to the iconic descending layers of winds of opposite sign (Fig. 1a). Opposing the down-

ward progression is tropical upwelling[17] from the Brewer-Dobson circulation[18]. It was thought, at least until recently, that horizontally propagating waves from the mid-latitudes into the tropics played only a minor part in the QBO's evolution[19] - explaining the QBO's remarkable cycle-to-cycle consistency with predictability extending out to a few years[16]. Indeed this consistency together with the oscillation's deep vertical structure allows 90% of the month-to-month variability of the QBO to be described by just two modes of variability known as Empirical Orthogonal Functions, or EOFs[20] (Methods).

Conventional QBO wisdom was challenged in February 2016 when its regular cycling was disrupted[4–6,21] for the first time since its discovery in the early 1960s[2,3]. A vertically thin layer of westward winds appeared at 40 hPa, within a decaying eastward QBO phase. Anomalous westward acceleration resulted from unusually large horizontal fluxes of wave-momentum from the Northern Hemisphere (NH)[5], linked to the occurrence of a very large El Niño event[21,22]. Conditions in the subtropics contributed to focusing the wave activity into the QBO jet[23,24]. Failures by models to predict the disruption[5] are consistent with it originating in the extra-tropics since predictability timescales are shorter there than in the tropics. The abnormal westward winds at 40 hPa subsequently strengthened, descended, and the QBO returned to its usual cycling by early 2017.

A second major QBO disruption, strongly resembling that of 2015/16, began in late-2019 and has persisted to the present (Fig. 1a). Here we determine those robust underlying mechanisms driving both disruptions. We directly assess the hypothesis that recurring QBO disruptions represent an emerging signal of climate change as opposed to natural variability that is currently difficult to quantify due to the short data record (just 28 QBO cycles). We also identify the implications the two disruptions have on predictability.

Disruptions to regular QBO cycling

The characteristic QBO descending eastward and westward wind pattern disintegrates in 2019/20 with unexpected westward winds appearing near 40 hPa along with an atypical ascending layer of eastward winds (Fig. 1a). The small vertical scale of the ascending eastward layer is unique in the QBO record. A decomposition of the QBO winds into EOFs (Methods) quantifies this unusual vertical structure (Fig. 1b). Whereas the first two EOFs (encompassing the largest scale downward propagating structure of the

QBO) typically explain over 90% of the vertical structure variance their values drop catastrophically to ∼20% by May 2020 as the higher order, smaller scale, EOFs 3 and 4 grow in amplitude. This extreme 2019/20 decrease in the variance explained by EOFs 1 and 2 greatly exceeds the decrease to 60% associated with the 2015/16 disruption.

Similarities and differences between the two disruptions become clearer from the zonal-mean zonal winds (Fig. 2a,b). Relative to the seasonal cycle the QBO phase evolution in 2019/20 is roughly 6 months ahead of that seen in 2015/16, with the eastward phase starting to recede during SH winter rather than NH winter. Similarly, the vertical wind shear at ∼50 hPa weakens and becomes westward in September 2019 compared to November 2015 (Fig. 2b). In both cases the westward vertical shear anomalies strengthened throughout the NH winter and preceded the emergence of corresponding 40 hPa westward wind anomalies by about 3 months (Fig. 2b), though in 2019/20 they emerge at a slightly lower altitude (43 hPa) than in 2015/26 (41 hPa).

Mechanisms

For both disruptions westward wave-forcing by meridional momentum transport (meridional EP-flux; Methods) was the main reason for the winds in the lower stratosphere (∼40 hPa) changing from eastward to westward (solid red line in Fig. 2c,d). From June to September 2019 the westward forcing from the meridional EP-flux is the largest single forcing term and opposes the more usual eastward forcing from the vertical-EP flux (dashed red line in Fig. 2c) expected during this phase of the QBO. This leads to very weak eastward winds that persist until January 2020 when the contribution from the meridional EP-flux strengthens again before the emergence of 40 hPa westward winds. In contrast during the 2015/2016 disruption there was a single period of strong forcing from the meridional EP Flux during the northern winter (December-March) leading up to the emergence of westward winds at 40 hPa (red line in Figure 2d).

Once the abnormal westward winds appear the forcing in both cases returns to the more established pattern of a balance between vertical advection and forcing from the vertical EP-flux (blue and red dashed lines in Figure 2c & d, respectively), consistent with an eventual return to the more usual QBO cycling. The key difference between the two events, then, was in the timing of the strongest forcing by horizontal waves: during

SH midwinter for the 2019/20 disruption, and during NH midwinter for the 2015/16 disruption.

Role of Southern Hemisphere in 2019/20 disruption

The SH winter of 2019 was unusual in that a sudden stratospheric warming (SSW) occurred, beginning in late August[25]. Only one other SSW is known to have occurred in the SH, during September 2002[26,27]. The timing of the 2019 SH SSW coincided with large westward forcing by meridional EP-flux and vertical advection that occurred in August–September (Fig. 2c), initiating the weak vertical shear anomaly that eventually developed into the westward disruption (Fig. 2a). The overturning circulation induced by the SSW[28] most likely accounts for increased forcing of the QBO by vertical advection in September 2019 (Fig. 2c).

Large forcing by horizontally propagating waves began in June 2019 (Fig. 2c) with the winter averaged (June–August) horizontal momentum flux reaching the equator at ∼40 hPa from the SH in 2019 the largest in the ERA5 record (Fig. 3a). Similarly, the largest winter averaged (December–February) horizontal momentum flux reaching the equator from the NH occurred during the 2015/16 QBO disruption. In contrast, the October–December momentum flux from the SH was not exceptional in 2019 compared to other years (not shown), even though persistent forcing by these waves continued to decelerate the already-weakened QBO eastward phase (Fig. 2c). Hence for both disruptions it appears that horizontal momentum fluxes initiated a weakening of the QBO eastward winds and development of the anomalous westward jet at 40 hPa roughly 3 months later. However, in contrast to the 2015/16 disruption, exceptional horizontal momentum fluxes for the 2019/20 disruption occurred well before the anomalous westward winds actually appeared, and originated from the SH rather than the NH.

The waves contributing to the SH fluxes in 2019 were ∼ 60% planetary scale (zonal wavenumbers k = 1–3) during June–July but in August at the levels where westward shear first appears (near 50 hPa, Fig. 2a) ∼ 60% came from synoptic scale waves (k = 4–10; not shown). Westward winds were present at most longitudes in the subtropics at this time, but in the 120° W–0° sector the wind was eastward (Fig. 3b) with strength of 5–10 m s^{-1} over most of the sector, similar to the strength of the zonal-mean QBO jet at this time (Fig. 2c). Large horizontal synoptic-scale momentum fluxes occurred within

this subtropical corridor of eastward winds, leading to abnormally large westward momentum flux convergence in the deep tropics (Fig. 3b); a similar mechanism appears to have been operative during the 2019/20 disruption[29]. The subtropical corridor occurs at roughly the same longitudes where the SH polar vortex was displaced equatorward toward South America, suggesting it was related to the developing SSW event.

An emerging eastward jet

Finally, a distinct feature of the 2019/20 disruption, contributing to its very unusual nature as quantified by Figure 1b, is the emergence of eastward zonal-mean zonal winds on the upper flank of the 40 hPa westward layer (Fig. 2a). This appears to have been forced by vertically propagating waves, and hence is more consistent with the conventional QBO paradigm than the westward disruption. Above 30 hPa prior to December 2019, vertical EP-flux was driving the descent of the QBO westward phase (Fig. 4a). After December 2019 this westward forcing gradually diminishes, consistent with increasing wave filtering by the strengthening westward winds below (Fig.4b). With less wave forcing to counteract vertical advection, the westward QBO phase descent stalls and then reverses. (A similar stall and reversal of westward phase descent occurred from December 2015 onward at higher altitudes, above 20 hPa, during the previous disruption; Figure 2b.) Increasing eastward shear on the upper flank of the westward disruption (Fig. 2a) is then accompanied by increasing eastward forcing by vertical EP-flux, leading to the emergence of eastward zonal-mean winds near 25 hPa in May 2020 (Fig. 4). Fourier decomposition reveals that ∼50% of this forcing is due to large-scale waves ($k = 1$–10; not shown), consistent with radiative damping of Kelvin waves as they encounter eastward zonal-mean wind shear. The rapid (sub-monthly) variations seen in Singapore observations in this region (Fig. 1a) are also consistent with Kelvin wave activity[30].

Discussion and Outlook

The quasi-biennial oscillation has been disrupted again, four years after the previous disruption, and for only the second time since its discovery. The two westward disruptions are similar, both occurring near 40 hPa and linked with historically large forcing from extratropical waves. However the 2019/20 event is different in that wave disturbances originated from the SH rather than the NH, no concurrent El Niño event was present, and an eastward jet subsequently emerged above the westward layer.

The SH winter of 2019 and the following NH winter were unique in several respects. The smallest Antarctic ozone hole in over 40 years resulted from elevated polar stratosphere temperatures following the September 2019 SSW[9]. In contrast, very low NH polar temperatures during February 2020 were associated with record Arctic ozone loss[31]. These NH conditions were linked to anomalously low Rossby wave activity and a strong polar vortex[7]. Taken together it is difficult to reconcile how the 2020 QBO disruption could have occurred without the SH wave contributions, which contrasts with the role of NH Rossby wave driving during the 2016 disruption[5,6,22].

The occurrence of two QBO disruptions in close succession naturally raises the question of whether these events are harbingers of systematic changes in stratospheric circulation. Radiosonde observations show long-term weakening of the QBO amplitude in the lowermost tropical stratosphere[10] and similar weakening is projected by models[11,12]. If weaker QBO winds are more easily disrupted, which is consistent with the occurrence of both disruptions during decaying eastward QBO phases, then the QBO may become increasingly susceptible to disruption in the future as its amplitude weakens, though the weakening amplitudes themselves may also be a manifestation of more frequent disruptions. Models also project an equatorward shift of critical surfaces for synoptic-scale Rossby waves[32], and since these waves played a role in both 2015/16[29,33] and latest disruptions, future increases in their equatorward propagation could also increase the likelihood of QBO disruptions. However these projected changes are accompanied by extremely large natural variability (cf. Fig. 3a) and so the observed record should be interpreted cautiously.

The 2019/20 QBO disruption suggests that the 2015/16 one – which at the time could be seen as a rare event, occurring during an extreme El Niño – may be more common than previously thought. Predicting the evolution of the 40 hPa westward layer, and the emerging eastward jet above it, will prove a stringent test of models. Such work will be aided by the availability of new Aeolus satellite wind observations that will monitor the evolution of the QBO over the whole tropical belt in the coming months[34]. However, the increased influence of the extratropics on the QBO identified here suggests that tropical stratospheric winds could become less predictable in future, leading to less skilful seasonal forecasts.

Methods

Our characterization of the QBO disruption is based on a tropical rawinsonde station (Singapore, 1°N, 103°E) and global gridded analysis fields (ERA5 reanalysis[35] and ECMWF operational analysis (OA)[36,37]).

Daily and monthly averages of the zonal wind component were constructed from the twice daily meteorological Singapore soundings[38]. The vertical structure (100–10 hPa) of the QBO was decomposed into a set of Empirical Orthogonal Functions (EOFs[20,21]) based on the monthly averages from Jan 1976–Dec 2014. The monthly winds from Jan 2013–May 2020 were then projected onto the first four leading EOFs as the Principal Components (PCs) and the relative variance explained by each of the PCs calculated for each month.

The ERA5 reanalysis combines a global atmospheric model with surface, aircraft, and satellite observations from 1979-present, resulting in an ongoing global, gridded, data set of winds and temperature that captures tropospheric weather systems, stratospheric waves and circulations, and the QBO[35]. These gridded meteorological fields (6-hourly in time, 2° horizontal and ∼0.5 km vertical) are used to calculate contributions to the zonal-mean zonal momentum budget due to wave forcing, quantified by the Eliassen-Palm (EP) flux, and advection[39]. Note that for these calculations the high vertical resolution model levels are used as reanalysis output on the standard available pressure levels have insufficient vertical resolution for accurate calculation of vertical wind shear and other vertical gradients involved in the momentum budget calculations.

An advantage of reanalyses over operational analyses used by weather forecasting centres is that the forecast model and data assimilation methodology are fixed for the whole reanalysis duration enabling consistent comparison of the 2015/16 and 2019/20 disruptions. However, we complement ERA5 with ECMWF OA so as to extend the data record to near-present day, since the availability of ERA5 model levels data on the Copernicus Data Store lags real time by approximately two months.

Acknowledgments

ERA5 data were obtained from the Copernicus Data Store. The European Centre for Medium-Range Weather Forecasts (ECMWF) Operational Analysis data were ob-

tained via the online portal (www.ecmwf.int/en/forecasts). The Singapore soundings were obtained from the NOAA IGRA2 data center. NB was supported by the Met Office Hadley Centre Programme funded by BEIS and Defra. LC was supported by the NASA Modeling and Analysis Program. PN was supported by the NASA Atmospheric Composition Modeling and Analysis Program. SO was supported by the National Centre for Atmospheric Science and UK NERC (NE/P006779/1, NE/N018001/1). CW was funded by the Royal Society, University Research Fellowship (UF160545). TB was funded by an EPSRC Doctoral Training Account.

Author Contributions

JA, NB, LC, PN and SO designed the study, performed the analysis and drafted the paper. TB and CW provided input on wind observations and their interpretation.

References

1. Baldwin, M. P. *et al.* The quasi-biennial oscillation. *Rev. Geophys.* **39,** 179–229 (2001).
2. Ebdon, R. & Veryard, R. Fluctuations in equatorial stratospheric winds. *Nature* **189,** 791–793 (1961).
3. Reed, R. J., Campbell, W. J., Rasmussen, L. A. & Rogers, D. G. Evidence of a downward-propagating, annual wind reversal in the equatorial stratosphere. *Journal of Geophysical Research* **66,** 813–818 (1961).
4. Newman, P. A., Coy, L., Pawson, S. & Lait, L. R. The anomalous change in the QBO in 2015–2016. *Geophysical Research Letters* **43,** 8791–8797 (2016).
5. Osprey, S. M. *et al.* An unexpected disruption of the atmospheric quasi-biennial oscillation. *Science* **353,** 1424–1427 (2016).
6. Coy, L., Newman, P. A., Pawson, S. & Lait, L. R. Dynamics of the Disrupted 2015/16 Quasi-Biennial Oscillation. *Journal of Climate* **30,** 5661–5674 (2017).
7. Newman, P., Nash, E. & Pawson, S. *Annual Meteorological Statistics for the Northern Hemisphere* 2020. `https://acd-ext.gsfc.nasa.gov/Data_services/met/ann_data.html#ncep_clim_stats_nh` (2020).
8. Farman, J., Gardiner, B. & Shanklin, J. Large losses of total ozone in Antarctica reveal seasonal ClOx/NOx interaction. *Nature* **315,** 207–210 (1985).

9. Newman, P. & Nash, E. *NASA Ozone Watch: Annual Records* 2020. `https://ozonewatch.gsfc.nasa.gov/statistics/annual_data.html` (2020).
10. Kawatani, Y. & Hamilton, K. Weakened stratospheric quasibiennial oscillation driven by increased tropical mean upwelling. *Nature* **497,** 478 (May 2013).
11. Butchart, N. *et al.* QBO Changes in CMIP6 Climate Projections. *Geophysical Research Letters* **47,** e2019GL086903 (2020).
12. Richter, J. H. *et al.* Response of the Quasi-Biennial Oscillation to a warming climate in global climate models. *Quarterly Journal of the Royal Meteorological Society* **n/a** (2020).
13. Tegtmeier, S. *et al.* Temperature and tropopause characteristics from reanalyses data in the tropical tropopause layer. *Atmospheric Chemistry and Physics* **20,** 753–770 (2020).
14. Bushell, A. C. *et al.* Evaluation of the Quasi-Biennial Oscillation in global climate models for the SPARC QBO-initiative. *Quart. J. Roy. Meteor. Soc.* **Accepted** (2020).
15. Anstey, J. A. & Shepherd, T. G. High-latitude influence of the quasi-biennial oscillation. *Quarterly Journal of the Royal Meteorological Society* **140,** 1–21 (2014).
16. Scaife, A. A. *et al.* Predictability of the quasi-biennial oscillation and its northern winter teleconnection on seasonal to decadal timescales. *Geophysical Research Letters* **41,** 1752–1758 (2014).
17. Dunkerton, T. J. The role of gravity waves in the quasi-biennial oscillation. *Journal of Geophysical Research: Atmospheres* **102,** 26053–26076 (1997).
18. Butchart, N. The Brewer-Dobson circulation. *Reviews of Geophysics* **52,** 157–184 (2014).
19. O'Sullivan, D. Interaction of extratropical Rossby waves with westerly quasi-biennial oscillation winds. *Journal of Geophysical Research: Atmospheres* **102,** 19461–19469 (1997).
20. Wallace, J. M., Panetta, R. L. & Estberg, J. Representation of the equatorial stratospheric quasi-biennial oscillation in EOF phase space. *J. Atmos. Sci.* **50,** 1751–1762 (1993).
21. Dunkerton, T. J. The quasi-biennial oscillation of 2015–2016: Hiccup or death spiral? *Geophysical Research Letters* **43,** 10, 547–10, 552 (2016).

22. Barton, C. A. & McCormack, J. P. Origin of the 2016 QBO Disruption and Its Relationship to Extreme El Niño Events. *Geophysical Research Letters* **44,** 11, 150–11, 157 (2017).

23. Hitchcock, P., Haynes, P. H., Randel, W. J. & Birner, T. The emergence of shallow easterly jets within QBO westerlies. *Journal of the Atmospheric Sciences* **75,** 21–40 (2018).

24. Watanabe, S., Hamilton, K., Osprey, S., Kawatani, Y. & Nishimoto, E. First Successful Hindcasts of the 2016 Disruption of the Stratospheric Quasi-biennial Oscillation. *Geophysical Research Letters* **45,** 1602–1610 (2018).

25. Yamazaki, Y. *et al.* September 2019 Antarctic sudden stratospheric warming: quasi-6-day wave burst and ionospheric effects. *Geophysical Research Letters* **47** (2020).

26. Newman, P. A. & Nash, E. R. The unusual Southern Hemisphere stratosphere winter of 2002. *Journal of the Atmospheric Sciences* **62,** 614–628 (2005).

27. Butler, A. H., Sjoberg, J. P., Seidel, D. J. & Rosenlof, K. H. A sudden stratospheric warming compendium. *Earth System Science Data* **9,** 63–76 (2017).

28. Baldwin, M. P. *et al.* Sudden Stratospheric Warmings. *Earth and Space Science Open Archive,* 49 (2020).

29. Lin, P., Held, I. & Ming, Y. The Early Development of the 2015/16 Quasi-Biennial Oscillation Disruption. *Journal of the Atmospheric Sciences* **76,** 821–836 (2019).

30. Hendon, H. H. & Wheeler, M. C. Some space–time spectral analyses of tropical convection and planetary-scale waves. *Journal of the atmospheric sciences* **65,** 2936–2948 (2008).

31. Lindsay, R. *Spring 2020 brings rare ozone "hole" to the Arctic* `https://www.climate.gov/news-features/event-tracker/spring-2020-brings-rare-ozone-%E2%80%9Chole%E2%80%9D-arctic` (2020).

32. Shepherd, T. G. & McLandress, C. A Robust Mechanism for Strengthening of the Brewer–Dobson Circulation in Response to Climate Change: Critical-Layer Control of Subtropical Wave Breaking. *Journal of the Atmospheric Sciences* **68,** 784–797 (2011).

33. Li, H., Kedzierski, R. P. & Matthes, K. On the forcings of the unusual QBO structure in February 2016. *Atmospheric Chemistry and Physics Discussions* **2019,** 1–31 (2019).

34. Witschas, B. *et al.* First validation of Aeolus wind observations by airborne Doppler Wind Lidar measurements. *Atmospheric Measurement Techniques Discussions,* 1–23 (2020).

35. Hersbach, H. *et al.* The ERA5 global reanalysis. *Quarterly Journal of the Royal Meteorological Society* (2020).

36. Dee, D. P. *et al.* The ERA-Interim reanalysis: Configuration and performance of the data assimilation system. *Quarterly Journal of the royal meteorological society* **137,** 553–597 (2011).

37. NCAS British Atmospheric Data Centre. *European Centre for Medium-Range Weather Forecasts: ECMWF operational analysis: Assimilated Data* 2006. `http://catalogue.ceda.ac.uk/uuid/c46248046f6ce34fc7660a36d9b10a71` (2020).

38. Durre, I., Xungang, Y., Vose, R. S., Applequist, S. & Arnfield, J. Integrated Global Radiosonde Archive (IGRA), Version 2. *NOAA National Centers for Environmental Information* (Accessed May 2020. 2016).

39. Andrews, D. G., Holton, J. R. & Leovy, C. B. *Middle Atmosphere Dynamics* (Academic, San Diego, Calif., 1987).

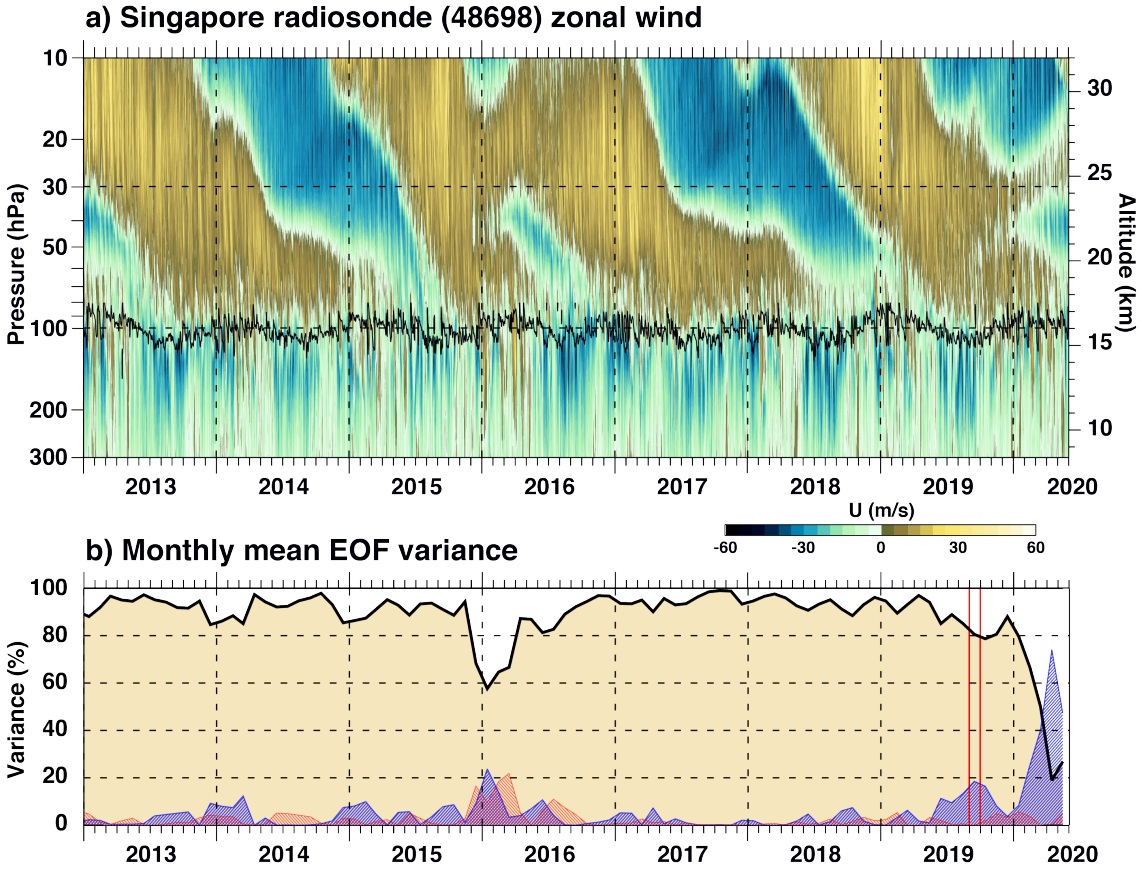

Figure 1. a) Twice daily radiosonde zonal wind observed at Singapore (1.4° N, 104° E, station id 48698). Lapse-rate tropopause determined from the radiosonde temperatures is shown as a black line. Missing radiosonde data are filled in with MERRA-2 interpolated to the location of Singapore. b) The percent variance explained by principal components (PCs) 1 and 2 combined (black curve) and PCs 3 (red curve) and 4 (blue curve) as a function of time based on the monthly averaged Singapore zonal wind profiles (1976–2020) from 100–10 hPa. The EOF calculation was based on monthly averaged winds limited to 1976–2014 to avoid the two disruptions. The red vertical lines bracket September 2019.

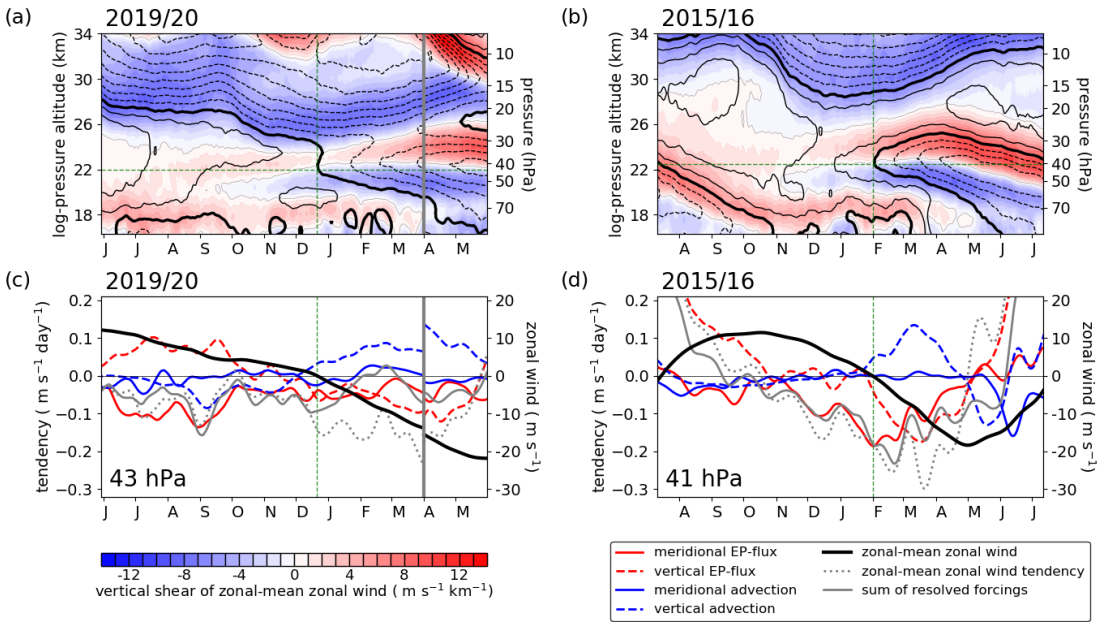

Figure 2. QBO disruptions as seen in the ERA5 reanalysis during (a,c) 2019/20 and (b,d) 2015/16. (a,b) Zonal-mean zonal wind (black contours; zero thick, westward dashed, 5 m s^{-1} spacing) and its vertical shear (filled contours). (c,d) Zonal-mean zonal wind tendency due to eddy momentum transports and advection, and zonal-mean zonal wind (thick black line). Vertical green dashed lines marks the time when westward winds first emerge near 40 hPa for each disruption. Horizontal green dashed lines in (a,b) indicate the altitudes shown in (c,d) respectively. All panels use daily ERA5 daily, 4° S–4° N average, smoothed with (a,b) 5-day running mean, (c,d) 31-day running mean. For the 2019/20 disruption, ERA5 data are extended in time using ECMWF operational analysis (transition marked by grey vertical line in panels a, c).

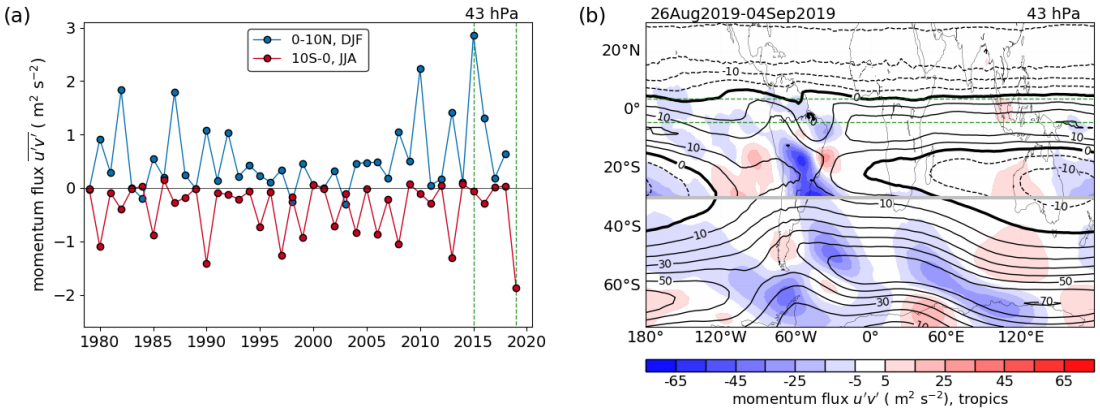

Figure 3. (a) Zonal-mean horizontal eddy momentum flux at 43 hPa, ERA5 reanalysis averaged over 0° –10° N during NH midwinter (December–February, DJF) and 10° S–0° during SH midwinter (June–August, JJA). Vertical green dashed lines mark the years of the two QBO disruptions, 2015/16 and 2019/20 (for the DJF mean, the year on horizontal axis indicates the year of the December). (b) Horizontal eddy momentum flux (filled contours) and zonal wind (line contours; zero thick, westward dashed) at 43 hPa, ERA5 reanalysis, averaged over 10 days when forcing of equatorial wind by meridionally propagating waves peaks for the 2019/20 disruption (Figure 2d, red solid line). Different contour values are shown for the tropics and extratropics (break is at 30° S, grey line): momentum flux contours have 10× larger spacing in the extratropics, and wind contours have 2× larger spacing. Horizontal green dashed lines mark the 4° S–4° N range used to define the QBO wind in Figure 2.

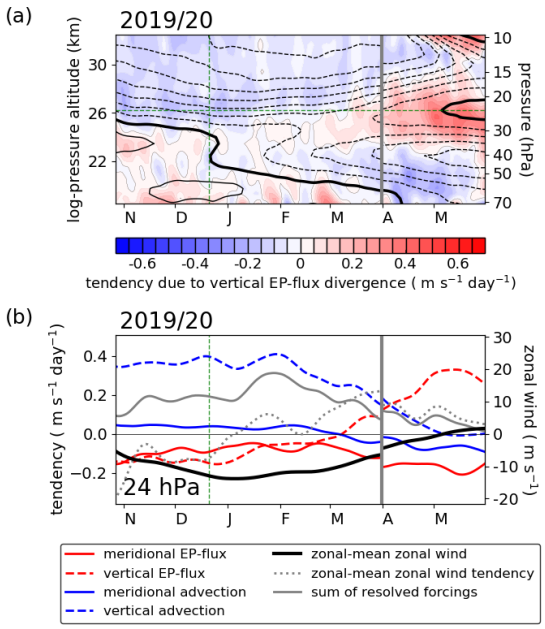

Figure 4. (a) Zonal-mean zonal wind (black contours; zero thick, westward dashed, 5 m s^{-1} spacing) and wind tendency due to vertical EP-flux component (filled contours). (b) Zonal-mean zonal wind tendency due to eddy momentum transports and advection, and zonal-mean zonal wind (thick black line), at the altitude of emerging eastward winds. Vertical green dashed line marks the time when westward winds first emerge near 40 hPa. Horizontal green dashed line in (a) indicates the altitude shown in (b). All panels use daily ERA5 daily, 4° S–4° N average, smoothed with (a) 11-day running mean, (b) 31-day running mean. ERA5 data are extended in time using ECMWF operational analysis (transition marked by grey vertical line in panels a, b).